RESEARCH ARTICLE

Editorial Process: Submission:03/09/2025 Acceptance:02/26/2026 Published:02/07/2026

Mitogen-Activated Protein Kinase-3 (MAPK3) Is the Main Target of Microsecond Pulsed Electric Field in Human Medulloblastoma

Ayad Bahadorimonfared[1], Zahra Razzaghi[2]*, Reza M Robati[3], Babak Arjmand[4,5], Naybali Ahmadi[6], Nastaran Asri[7], Aliasghar Keramatinia[8], Farideh Razi[9], Fatemeh Bandarian[10]

Abstract

Introduction: Pulsed electric fields (PEFs) are applied to facilitate the transfer of various types of molecules, such as pharmaceuticals, into living cells. In the present study effect of microsecond PEF on human medulloblastoma cell line (D283Med cells) is investigated to find the crucial targeted genes. **Methods:** Gene expression profiles of the human medulloblastoma (D283) cell line in response to microsecond PEF versus control are extracted from the Gene Expression Omnibus (GEO) database. The samples are analyzed via the GEO2R program to find the significant differentially expressed genes (DEGs). The significant DEGs were assessed via protein-protein interaction (PPI) network using Cytoscape software and its applications. **Results:** Among 410 significant DEGs, 23 hubs and bottlenecks were determined. A total number of seven hub-bottlenecks including MAPK3, KIT, APP, RUNX2, CXCR4, LMNA, and BMP4 were pointed out as the crucial targets of microsecond PEF. MAPK3 and KIT were down-regulated while, APP, RUNX2, CXCR4, LMNA, and BMP4 were up-regulated. **Conclusion:** It can be concluded that, down-regulation of MAPK3 and KIT and up-regulation of BMP4 which are the consequence of microsecond PEF treatment inhibit medulloblastoma. The results exhibited the significant role of MAPK3 in response to microsecond PEF treatment.

Keywords: Microsecond pulsed electric field; Medulloblastoma; Network analysis, Human, Cell

Asian Pac J Cancer Prev, **27 (2)**, 463-468

Introduction

Various pulsed electric fields are a suitable tool to facilitate the transfer of different type of molecules, such as pharmaceuticals, into living cells [1]. Experiences have shown that PEF-based technologies are able to treat cancer. These methods in two ways can be used: first direct biological effect of PEFs and the second; the cytotoxicity of genes productions under effect of applied PEFs [2]. Tanori M et al. used microsecond pulsed electric fields to explore the response of the human medulloblastoma cell line (D283Med cells). Based on this investigation, the applied specific pulse protocol irreversibly changed membrane permeability and induced apoptosis in the treated cells [3]. Stacey M et al. published data about the effect of nanosecond PEFs on various human cell lines. They have reported that chromosomal telomere damage, nuclear membrane injury, and cell cytoskeleton breakdown were happened in the treated cells [4].

Detection of the molecular mechanism of diseases and therapeutic methods has gained significant reputation in the control of diseases and disorders [5, 6]. Large-scale tools, such as genomics and proteomics play a crucial role to exploring the molecular mechanism of diseases.

*[1]Department of Health & Community Medicine, Faculty of Medicine, Shahid Beheshti University of Medical Sciences, Tehran, Iran. [2]Laser Application in Medical Sciences Research Center, Shahid Beheshti University of Medical Sciences, Tehran, Iran. [3]Skin Research Center, Shahid Beheshti University of medical sciences, Tehran, Iran. [4]Cell Therapy and Regenerative Medicine Research Center, Endocrinology and Metabolism Molecular-Cellular Sciences Institute, Tehran University of Medical Sciences, Tehran, Iran. [5]Iranian Cancer Control Center (MACSA), Tehran, Iran. [6]Proteomics Research Center, System Biology Institute, Faculty of Paramedical Sciences, Shahid Beheshti University of Medical Sciences, Tehran, Iran. [7]Celiac Disease and Gluten Related Disorders Research Center, Research Institute for Gastroenterology and Liver Disease, Shahid Beheshti University of Medical Sciences, Tehran, Iran. [8]Department of Community Medicine, School of Medicine, Shahid Beheshti University of Medical Sciences, Tehran, Iran. [9]Diabetes Research Center, Endocrinology and Metabolism Clinical Sciences Institute, Tehran University of Medical Sciences, Tehran, Iran. [10]Endocrinology and Metabolism Research Center, Endocrinology and Metabolism Clinical Sciences Institute, Tehran University of Medical Sciences, Tehran, Iran. *For Correspondence: z.razaghi@gmail.com*

Zamanian–Azodi M et al. suggested a biomarker panel for esophageal cancer via a proteomics method [7]. Abbaszadeh HA et al. investigated proteome alteration of human gingival fibroblast cells in response to laser radiation. They showed that the Er: YAG laser affected cell cycle regulation of human gingival fibroblast cells [8]. Due to the complexity of genomic data, using bioinformatics for the interpretation of genomic findings is a common manner [9, 10]. Protein-protein interaction network analysis as a bioinformatics approach is a suitable method to screen gene or protein sets [11]. Interacting genes have a special position in the interactome. The genes that connect to large numbers of neighbors are known as hub genes. These hub genes play a critical role in the network. The other central genes are bottleneck genes; the genes that participate in many shortest paths. The common hub and bottleneck genes are known as hub-bottlenecks. It is reported that the hub-bottleneck genes are the crucial nodes of the constructed network [12-14]. In the present study, gene expression alteration of the human medulloblastoma (D283) cell line in response to microsecond PEF is extracted from the GEO database. Data are investigated via PPI network analysis to find the crucial molecular events to evaluate the anticancer property of the applied microsecond PEF on the treated human cancer cell line.

Materials and Methods

Data collection

The Effect of a microsecond pulsed electric field on gene expression of the human medulloblastoma (D283) cell line was searched in the GEO database. GSE248601 (https://www.ncbi.nlm.nih.gov/geo/geo2r/?acc=GSE248601) was explored as a suitable source to be analyzed. The medulloblastoma cells were exposed to 0.3 MV/m, 40 µs, 5 pulses of microsecond pulsed electric field. Details of methods are described in reports of Casciati A et al. [15]. Total RNA of samples was extracted after 24 hours from treatment using QIAzol and the miRNeasy Micro Kit from Qiagen.

Pre-evaluation analysis: The gene expression profiles were analyzed via GEO2R program to explore the significant DEGs. Uniform Manifold Approximation and Projection (UMAP) analysis was applied to compare the similarity of samples. A similar pattern of gene expression of samples was assessed via an Expression Density Plot. The significant DEGs were identified based on an adjusted p-value < 0.05. The genes IDs were decoded to official gene symbols and the uncharacterized individuals were ignored.

PPI network analysis: The significant DEGs were imported in "protein query" of STRING database via Cytoscape software v 3.7.2. To maximize interactions between the nodes, a confidence score 0.2 was applied. The PPI network was created via undirected edges and was analyzed via "Network Analyzer" plugin. The hubs of the main connected component of the PPI network were identified based on degree value > (mean+2 standard deviation) cutoff. The top Five percent of nodes, based on betweenness centrality were selected as bottleneck genes. The common hub-bottleneck nodes were pointed out as hub-bottlenecks. The hubs and bottleneck nodes were included in CluePedia plugin to form a directed network via Cytoscape software. The nodes were connected via activation, inhibition, expression, catalysis, reaction, and post translation modification actions. The hub-bottleneck nodes that were included in the main connected component of the directed PPI network were enriched for biological processes via ClueGO application of Cytoscape software.

Statistical analysis: The significant DEGs were selected based on an adjusted p-value < 0.05. The PPI network was formed using a confidence score of 0.2. The biological processes were determined based on the following criteria: Kappa score threshold=0.4, term p-value, term p-value corrected with the Bonferroni step-down, group p-value, and group p-value corrected with Bonferroni step- down less than 0.05. For further detail, "Network specificity" was applied. Redundant groups with more than 50% overlap were merged.

Results

To compare the gene expression profiles of the samples UMAP plot (Figure 1) was illustrated. The treated samples are completely separated from the controls. This finding corresponds to the difference between the radiated samples from control individuals. It can be expressed that the treatment affected gene expression activity of the cells. Similar patterns of gene expression in the treated and untreated cells are shown in Figure 2. This finding indicates that the gene expression profiles are comparable.

A total number of 410 significant DEGs were identified for more analysis. The main connected component of PPI network, including 402 nodes and 3,193 edges was created. The central part of the main connected component is illustrated in Figure 3. MAPK3, VEGFA, CAV1, KIT, APP, RUNX2, CXCR4, KLF4, BMP4, LMNA, HMOX1, VCL, ANXA1, RHOC, SPARC, and CSF1 were determined as hub genes. MAPK3, VEGFA, APP, CAV1, RUNX2, BRCA2, LMNA, PPARGC1A, KIT, ASPM,

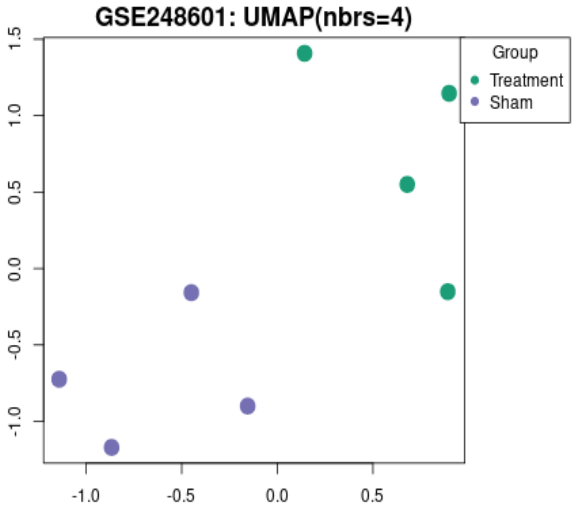

Figure 1. UMAP Plot Presentation of Treated Samples and the Controls Gene Expression Profiles. Each sample is compared with 4 its neighbors.

HMOX1, RHOC, ANXA1, TXNRD1, MERTK, BMP4, TFRC, CXCR4, GAS7, and SPARC were introduced as bottleneck DEGs. The list of hubs, bottlenecks, and hub-bottleneck genes is presented in Table 1.

The directed PPI network is shown in the Figure 4. As depicted in Figure 4, except CSF1, all element of the main connected component (MAPK3, KIT, APP, RUNX2, CXCR4, LMNA, BMP4, ANXA1, SPARC) are hub-bottleneck genes. These genes were enriched via gene ontology to explore the related biological processes (see Figure 5). As depicted in Figure 5, 7 groups of biological processes are related to 7 hub-bottleneck of the main connected component of the directed PPI network.

Discussion

Pre-evaluation analysis showed the applied PEF effectively changed the gene expression profile of the

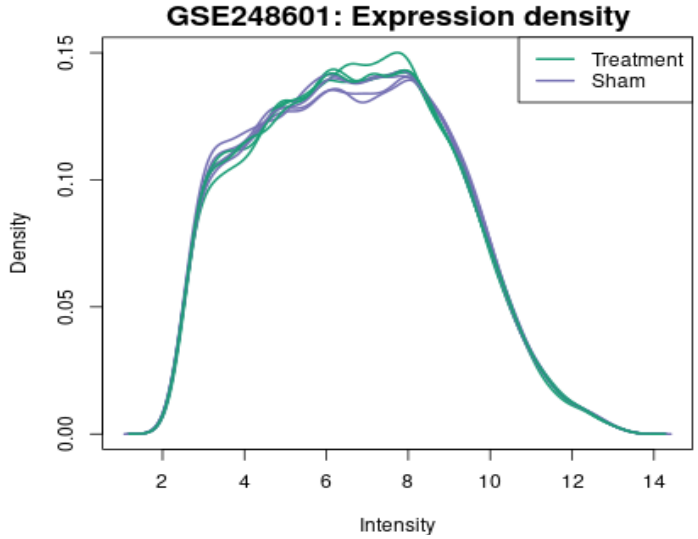

Figure 2. Expression Density Plot Presentation of Treated Cells and the Controls Gene Expression Profiles

Table 1. List of Hubs, Bottleneck Nodes, and Hub-Bottleneck DEGs. The superscripted letters h and b are corresponded to hub and bottleneck, respectively. the hub-bottleneck nodes are bold.

No.	display name	Degree	Betweenness centrality	Log (fold change)
1	**MAPK3**	115	0.083	-0.79
2	**VEGFA**	99	0.046	0.86
3	**CAV1**	76	0.036	-1.01
4	**KIT**	67	0.022	-1.04
5	**APP**	66	0.037	0.62
6	**RUNX2**	62	0.026	0.58
7	**CXCR4**	61	0.016	1.01
8	**LMNA**	55	0.024	1
9	**BMP4**	55	0.018	1.88
10	**HMOX1**	53	0.02	3.09
11	**RHOC**	50	0.02	0.43
12	**ANXA1**	50	0.02	5.1
13	**SPARC**	49	0.016	2
14	KLF4[h]	57	0.014	0.87
15	VCL[h]	53	0.015	0.51
16	CSF1[h]	46	0.006	1.54
17	PPARGC1A[b]	45	0.023	-0.7
18	TFRC[b]	45	0.017	0.61
19	BRCA2[b]	40	0.024	-0.75
20	TXNRD1[b]	40	0.019	0.57
21	ASPM[b]	36	0.021	-0.45
22	GAS7[b]	34	0.016	1.25
23	MERTK[b]	33	0.019	0.74

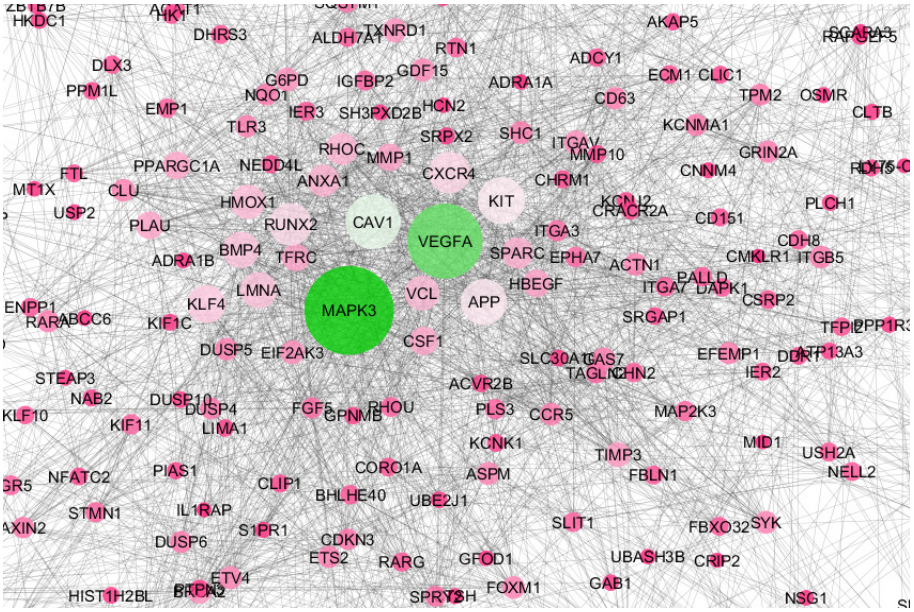

Figure 3. Central Part of the Main Connected Component of the Undirected PPI Network. The nodes are layout based on degree value.

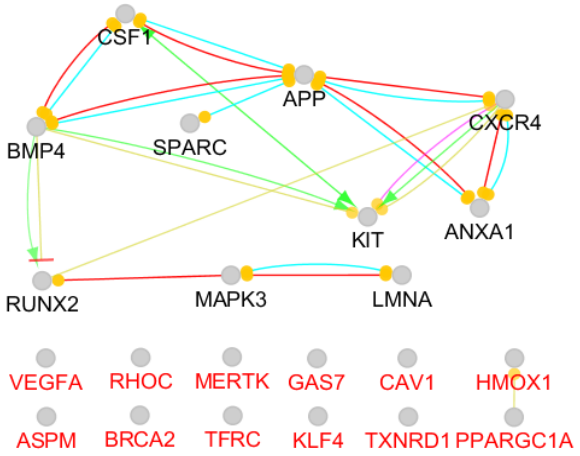

Figure 4. Action Map of the Hub and Bottleneck Genes. Blue yellow, red, pink, and green refer to reaction, expression, catalysis, post translation modification, and activation actions, respectively.

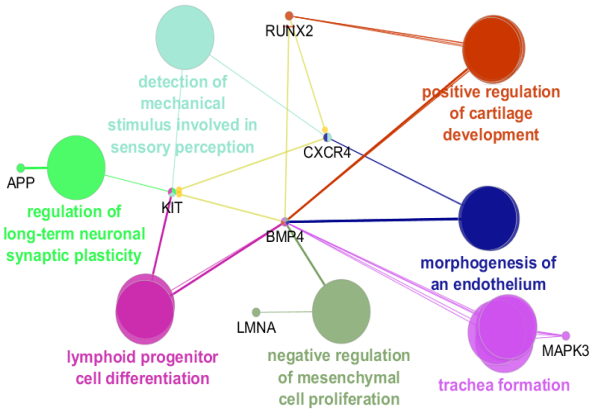

Figure 5. Biological Processes Related to the Hub-Bottleneck of the Main Connected Component of the Directed PPI Network. The associate DEGs are labeled in black.

treated D283 Med cells. Human brain tissue includes a large number of tissue-specific proteins and genes [16]. It seems that the results of gene expression profile change of the exposed D283 Med cells to PEF are valid for the other types of brain cancer. PPI network analysis and gene ontology enrichment showed that MAPK3, KIT, APP, RUNX2, CXCR4, LMNA, and BMP4 are the critically affected genes. As depicted in Table 1, MAPK3 and KIT are down-regulated while APP, RUNX2, CXCR4, LMNA, and BMP4 are up-regulated.

Mitogen-activated protein kinase-3 (MAPK3) is the top-ranked hub and bottleneck gene. It is down-regulated in response to the applied PEF. MAPK is known as a serine/threonine protein kinase which can be activated by various extracellular signal including cytokines, chemical and physical stress, and growth factors. It is associated with cell differentiation, proliferation, and transformation. The role of MAPK in apoptosis, inflammation, and other pathological and physiological processes in the body is highlighted in literature [17]. An investigation by MacDonald TJ et al. showed that a decrement of MAPK3 activation leads to inhibition of the metastatic potential of Daoy medulloblastoma cells [18]. KIT proto-oncogene, receptor tyrosine kinase (KIT), is another critical down-regulated DEGs. Heinrich MC et al. have suggested the KIT inhibition as a therapeutic method in the treatment of kit-positive malignancies [19]. Based on Blom T et al. investigation, co-amplification of platelet-derived growth factor receptor alpha along with KIT can be considered as a molecular biomarkers in medulloblastomas [20].

Amyloid-beta precursor protein (APP) is another critical up-regulated DEGs in response to PEF treatment.

APP is well-known associated gene with pathogenesis of Alzheimer's disease (AD) [21]. Wu Y et al. published document about inhibition of cell proliferation via over-expression of APP [22]. This finding was obtained via performed gene expression profiling using a microarray experiment in human cells. RUNX family transcription factor 2 (RUNX2) is the fourth crucial up-regulated DEGs. It is pointed out that RUNX2 plays significant role in modulating chondrocyte and osteoblast differentiation and hypertrophy [23]. RUNX2-mRNA levels were explored in glioblastoma tissues by Yamada D et al. [24]. Based on this document RUNX2-mRNA levels were higher in glioblastoma samples than the normal brains or low-grade gliomas. It is suggested that RUNX2 protein level is positively correlated with proliferative capacity of the cells. CXC chemokine receptor-4 (CXCR4) is the fifth key DEGs. Involvement of CXCR4 in hematopoiesis and cell homing, cell migration, and retention in the bone marrow is pointed out in literature [25]. Based on previous studies, CXCR4 is over-expressed in ovarian cancer, breast cancer, melanoma, small-cell lung cancer, brain cancers, hepatocellular carcinoma, pancreatic cancer, gastric and stomach cancers, and soft tissue sarcomas [26].

Prelamin-A/C (LMNA) is the sixth crucial DEGs. A significant increase in LMNA levels in the brain of Alzheimer disease patients was reported by Rosene MJ et al. [27]. Published reports have shown the role of LMNA in the progression and development of tumors [28]. The last gene is bone morphogenetic protein 4 (BMP4). BMP4 belongs to TGF-β cytokines superfamily, which is involved in cell differentiation, maturation and proliferation [29]. Liu DD et al. showed the regulatory effect of RUNX2 on osteoblast differentiation. This process is demonstrated via the BMP4 signaling pathway [30]. Eckhardt BL et al. investigation showed positive role of BMP4 on metastasis block in breast cancer. Based on this document BMP4 improves survival in patients with breast cancer [31]. These assessments showed that MAPK3 and KIT down-regulation and BMP4 up-regulation act as cancer-preventive events. While the up-regulation of APP, RUNX2, CXCR4, and LMNA can be considered as the side effects of PEF therapeutic method.

In conclusion, the applied pulsed electric field inhibits medulloblastoma via down-regulation of MAPK3 and KIT, and up-regulation of BMP4. MAPK3 emerged as the top-ranked hub and bottlenecks and its centrality parameters showed considerable differences relative to KIT and BMP4 (degree value of about two-fold and betweenness centrality about four-fold). It can be concluded that MAPK3 inhibition is the main tool to suppress medulloblastoma.

Author Contribution Statement

All authors contributed equally in this study.

Acknowledgements

None.

References

1. Novickij V, Rembiałkowska N, Kasperkiewicz-Wasilewska P, Baczyńska D, Rzechonek A, Błasiak P, et al. Pulsed electric fields with calcium ions stimulate oxidative alternations and lipid peroxidation in human non-small cell lung cancer. Biochimica et Biophysica Acta (BBA) - Biomembranes. 2022;1864(12):184055. https://doi.org/10.1016/j.bbamem.2022.184055.
2. Guo S, Sersa G, Heller R. Editorial: Pulsed electric field based technologies for oncology applications. Front Oncol. 2023;13:1183900. https://doi.org/10.3389/fonc.2023.1183900.
3. Tanori M, Casciati A, Zambotti A, Pinto R, Gianlorenzi I, Pannicelli A, et al. Microsecond pulsed electric fields: An effective way to selectively target and radiosensitize medulloblastoma cancer stem cells. Int J Radiat Oncol Biol Phys. 2021;109(5):1495-507. https://doi.org/10.1016/j.ijrobp.2020.11.047.
4. Stacey M, Fox P, Buescher S, Kolb J. Nanosecond pulsed electric field induced cytoskeleton, nuclear membrane and telomere damage adversely impact cell survival. Bioelectrochemistry. 2011;82(2):131-4. https://doi.org/10.1016/j.bioelechem.2011.06.002.
5. Noh JY, Yang Y, Jung H. Molecular mechanisms and emerging therapeutics for osteoporosis. Int J Mol Sci. 2020;21(20):7623. https://doi.org/10.3390/ijms21207623.
6. McGee SL, Hargreaves M. Exercise adaptations: Molecular mechanisms and potential targets for therapeutic benefit. Nat Rev Endocrinol. 2020;16(9):495-505. https://doi.org/10.1038/s41574-020-0377-1.
7. Zamanian-Azodi M, Rezaei-Tavirani M, Hasanzadeh H, Rahmati Rad S, Dalilan S. Introducing biomarker panel in esophageal, gastric, and colon cancers; a proteomic approach. Gastroenterol Hepatol Bed Bench. 2015;8(1):6-18.
8. Abbaszadeh HA, Peyvandi AA, Sadeghi Y, Safaei A, Zamanian-Azodi M, Khoramgah MS, et al. Er:Yag laser and cyclosporin a effect on cell cycle regulation of human gingival fibroblast cells. J Lasers Med Sci. 2017;8(3):143-9. https://doi.org/10.15171/jlms.2017.26.
9. Doyle RM, O'Sullivan DM, Aller SD, Bruchmann S, Clark T, Coello Pelegrin A, et al. Discordant bioinformatic predictions of antimicrobial resistance from whole-genome sequencing data of bacterial isolates: An inter-laboratory study. Microb Genom. 2020;6(2):e000335. https://doi.org/10.1099/mgen.0.000335.
10. Pereira R, Oliveira J, Sousa M. Bioinformatics and computational tools for next-generation sequencing analysis in clinical genetics. J Clin Med. 2020;9(1):132. https://doi.org/10.3390/jcm9010132.
11. Rezaei-Tavirani M, Rezaei-Tavirani M, Mansouri V, Mahdavi SM, Valizadeh R, Rostami-Nejad M, et al. Introducing crucial protein panel of gastric adenocarcinoma disease. Gastroenterol Hepatol Bed Bench. 2017;10(1):21-8.
12. Fox AD, Hescott BJ, Blumer AC, Slonim DK. Connectedness of ppi network neighborhoods identifies regulatory hub proteins. Bioinformatics. 2011;27(8):1135-42. https://doi.org/10.1093/bioinformatics/btr099.
13. Nithya C, Kiran M, Nagarajaram HA. Hubs and bottlenecks in protein-protein interaction networks. Methods Mol Biol. 2024;2719:227-48. https://doi.org/10.1007/978-1-0716-3461-5_13.
14. Asadzadeh-Aghdaee H, Shahrokh S, Norouzinia M, Hosseini M, Keramatinia A, Jamalan M, et al. Introduction of inflammatory bowel disease biomarkers panel using protein-protein interaction (ppi) network analysis. Gastroenterol Hepatol Bed Bench. 2016;9(Suppl1):S8-s13.

15. Casciati A, Taddei AR, Rampazzo E, Persano L, Viola G, Cani A, et al. Involvement of mitochondria in the selective response to microsecond pulsed electric fields on healthy and cancer stem cells in the brain. Int J Mol Sci. 2024;25(4). https://doi.org/10.3390/ijms25042233.
16. Zhang Y, Zhang K, Bu F, Hao P, Yang H, Liu S, et al. D283 med, a cell line derived from peritoneal metastatic medulloblastoma: A good choice for missing protein discovery. J Proteome Res. 2020;19(12):4857-66. https://doi.org/10.1021/acs.jproteome.0c00743.
17. Yu TT, Wang CY, Tong R. Erbb2 gene expression silencing involved in ovarian cancer cell migration and invasion through mediating mapk1/mapk3 signaling pathway. Eur Rev Med Pharmacol Sci. 2020;24(10):5267-80. https://doi.org/10.26355/eurrev_202005_21309.
18. MacDonald TJ, Brown KM, LaFleur B, Peterson K, Lawlor C, Chen Y, et al. Expression profiling of medulloblastoma: Pdgfra and the ras/mapk pathway as therapeutic targets for metastatic disease. Nat Genet. 2001;29(2):143-52. https://doi.org/10.1038/ng731.
19. Heinrich M, Blanke C, Druker B, Corless C. Heinrich mc, blanke cd, druker bj, corless clinhibition of kit tyrosine kinase activity: A novel molecular approach to the treatment of kit-positive malignancies. J clin oncol 20(6): 1692-1703. Review. J Clin Oncol. 2002;20:1692-703. https://doi.org/10.1200/JCO.20.6.1692.
20. Blom T, Roselli A, Häyry V, Tynninen O, Wartiovaara K, Korja M, et al. Amplification and overexpression of kit, pdgfra, and vegfr2 in medulloblastomas and primitive neuroectodermal tumors. J Neurooncol. 2010;97(2):217-24. https://doi.org/10.1007/s11060-009-0014-2.
21. Aydin D, Weyer SW, Müller UC. Functions of the app gene family in the nervous system: Insights from mouse models. Exp Brain Res. 2012;217(3-4):423-34. https://doi.org/10.1007/s00221-011-2861-2.
22. Wu Y, Zhang S, Xu Q, Zou H, Zhou W, Cai F, et al. Regulation of global gene expression and cell proliferation by app. Sci Rep. 2016;6(1):22460. https://doi.org/10.1038/srep22460.
23. Lin TC. Runx2 and cancer. Int J Mol Sci. 2023;24(8):7001. https://doi.org/10.3390/ijms24087001.
24. Yamada D, Fujikawa K, Kawabe K, Furuta T, Nakada M, Takarada T. Runx2 promotes malignant progression in glioma. Neurochem Res. 2018;43(11):2047-54. https://doi.org/10.1007/s11064-018-2626-4.
25. Bianchi ME, Mezzapelle R. The chemokine receptor cxcr4 in cell proliferation and tissue regeneration. Front Immunol. 2020;11:2109. https://doi.org/10.3389/fimmu.2020.02109.
26. Scala S, D'Alterio C, Milanesi S, Castagna A, Carriero R, Farina FM, et al. New insights on the emerging genomic landscape of cxcr4 in cancer: A lesson from whim. Vaccines (Basel). 2020;8(2):164. https://doi.org/10.3390/vaccines8020164.
27. Rosene MJ, Wen N, Li Z, Brase L, Hsu S, Cruchaga C, et al. Lmna-mediated nucleoskeleton dysregulation in alzheimer disease. Alzheimers Dement. 2021;17(S3):e054396. https://doi.org/10.1002/alz.054396.
28. Hu C, Zhou A, Hu X, Xiang Y, Huang M, Huang J, et al. Lmna reduced acquired resistance to erlotinib in nsclc by reversing the epithelial-mesenchymal transition via the fgfr/mapk/c-fos signaling pathway. Int J Mol Sci. 2022;23(21):13237. https://doi.org/10.3390/ijms232113237.
29. Setiawan AM, Kamarudin TA, Abd Ghafar N. The role of bmp4 in adipose-derived stem cell differentiation: A minireview. Front Cell Dev Biol. 2022;10:1045103. https://doi.org/10.3389/fcell.2022.1045103.
30. Liu DD, Zhang CY, Liu Y, Li J, Wang YX, Zheng SG. Runx2 regulates osteoblast differentiation via the bmp4 signaling pathway. J Dent Res. 2022;101(10):1227-37. https://doi.org/10.1177/00220345221093518.
31. Eckhardt BL, Cao Y, Redfern AD, Chi LH, Burrows AD, Roslan S, et al. Activation of canonical bmp4-smad7 signaling suppresses breast cancer metastasis. Cancer Res. 2020;80(6):1304-15. https://doi.org/10.1158/0008-5472.Can-19-0743.